Effective charges and their relation to collectivity and shell structure

A. Wolf[1,2] and R. F. Casten[2,3]
[1]*Nuclear Research Centre Negev, P.O. Box 9001, Beer Sheba 84-190, Israel*
[2]*Brookhaven National Laboratory, Upton, New York 11973*
[3]*Institut fur Kernphysik, Universitat zu Köln, Zulpicher Strasse 77, 5000 Koln 41, Germany*
(Received 18 May 1992)

Effective boson charges, e_π and e_ν, are extracted for isotopic chains of most elements from $Z=42$ to the actinides from analytic expressions derived in the interacting boson approximation. It is shown that, in *valence* space models, such effective charges carry an additional, physically intuitive interpretation, beyond the normal one of ensuring agreement of calculated electromagnetic transition rates with experiment. In valence models e_π and e_ν are approximately proportional to the derivatives of $M(E2{:}0_1^+ \rightarrow 2_1^+)$ with N_π and N_ν, respectively; that is, they are measures of the rate of change of collectivity. This feature allows one to disentangle the separate roles of protons and neutrons in the development of collectivity and exposes subtle effects originating in the valence p-n interaction. The results are striking. While for most elements, $e_\pi > e_\nu$ as expected, certain regions display anomalously large e_ν, and, sometimes $e_\nu/e_\pi > 1$. These effects are interpreted in terms of the p-n interaction and, in particular, in terms of its monopole component which acts to shift single particle energies and, thereby, can alter shell gaps and the effective size of the valence space of one kind of particle as a function of the number of the other. Very small values of e_ν near midshell are also interpreted in terms of the saturation of collectivity in such regions.

PACS number(s): 21.60.Ev, 21.60.Cs, 21.60.−n

I. INTRODUCTION

It is well known that the addition of valence nucleons to the closed shells of a nucleus is accompanied by the appearance of a nonspherical field and thus the presence of an additional quadrupole moment of the protons inside the closed shell. This quadrupole core polarization effect can be renormalized as an effective charge of the nucleons added to the core. An estimate of this effect can be obtained following Bohr and Mottelson [1] and noting that the induced quadrupole moment due to the disturbed field is of the order $ZQ_{\rm sp}/A$, where $Q_{\rm sp}$ is the single-particle quadrupole moment. Thus the effective charges of the proton and neutron are expected to be

$$e_p^{\rm eff} = \left[1+\frac{Z}{A}\right]e \ , \tag{1}$$

$$e_n^{\rm eff} = \frac{Z}{A}e \ , \tag{2}$$

respectively. According to this schematic model [1],

$$e_n^{\rm eff}/e_p^{\rm eff} = Z/(A+Z) \ . \tag{3}$$

Of course, in practical nuclear structure calculations, effective charges are introduced to mock up other simplifications such as the use of schematic interactions, special truncations of the space (even within the valence shell), and so on. In most nuclear models, effective charges are therefore a normalization factor on transition rates designed to achieve agreement with experiment.

Of course, this is true of valence space models as well, but here effective charges also play an additional, fundamentally different, role. As recently discussed [2] in a short summary of this work, to a good approximation, proton and neutron effective charges in valence space models (such as, but not limited to, the interacting boson approximation) are proportional to the *derivative* of the $E2$ transition matrix element with respect to the number of valence protons and neutrons, respectively. Therefore an experimental determination of these parameters can provide valuable information on the underlying nuclear structure and, in particular, on the separate and intertwined roles of protons and neutrons in the development of collectivity.

A straightforward way to determine $e_p^{\rm eff}, e_n^{\rm eff}$ is by measuring $E2$ transition probabilities $[B(E2)]$ values. These quantities can be related directly to the effective charges of the nucleons. (Another method to determine effective charges is from $\pi^\pm$ scattering amplitudes [3]. However, the lack of experimental data does not allow a systematic analysis using this method.)

Here we will focus on the use of $B(E2{:}2_1^+ \rightarrow 0_1^+)$ values since an extensive compilation [4] of about 280 of these $B(E2)$ values in even-even nuclei has recently become available. This compilation now makes possible the undertaking of a systematic analysis of effective charges across the periodic table.

In a recent work [5], Raman *et al.* have extracted e_n/e_p ratios by fitting $B(E2)$ experimental values by different simple models. However, since their interest was mainly to understand the gross features of the systematics, they included a rather large number of nuclei in one fit. While this procedure can give interesting results which are important for our understanding of the mass dependence of the quantities involved, it can obscure lo-

cal variations of the effective charges. These variations may contain very valuable information, especially concerning transitional regions, where nuclear shapes change rather rapidly as a function of mass.

It is the purpose of this paper to present the results of a detailed and systematic analysis of about 120 $B(E2)$ transition probabilities for even-even nuclei with $A > 90$.

Effective charges were extracted for isotopic chains of even-even nuclei of most elements with $Z > 40$ using various analytic formulas derived within the framework of the interacting boson approximation (IBA). The results show that the effective charges of the protons increase slowly and monotonically with A. However, the effective charges of the neutrons are found to increase considerably in the vicinity of closed shells and to decrease to very small values toward the middle of the major shells. These effects will be interpreted in terms of the respective roles of protons and neutrons in the onset of collectivity and of the residual p-n interaction.

II. ANALYTIC RELATIONS FOR $B(E2)$ TRANSITION PROBABILITIES IN EVEN-EVEN NUCLEI

In order to extract values of the effective charges from $B(E2)$ experimental data, we need a model that relates the $B(E2)$'s to e_p, e_n. A convenient model to use for this purpose is the IBA. In its dynamical symmetry limits, this model uses group algebra to derive analytic formulas for important nuclear observables. Since we are interested in effective charges of protons and neutrons, we will use IBA-2. A convenient Hamiltonian for IBA-2 is

$$H=\varepsilon(\hat{n}_{d_\nu}+\hat{n}_{d_\pi})+\kappa Q_\nu\cdot Q_\pi \ , \tag{4}$$

with

$$Q_{\pi,\nu}=(s^\dagger d+d^\dagger s)+\chi_{\pi,\nu}(d^\dagger d)^2 \ , \tag{5}$$

and $\hat{n}_d$ the d-boson number operator. The $E2$ transition operator has the form

$$T(E2)=e_\pi Q_\pi+e_\nu Q_\nu \ , \tag{6}$$

where e_π (e_ν) are the proton (neutron) boson effective charges. The transition probability $B(E2)$ is determined from the expectation value of $T(E2)$. For the three limiting symmetries of the IBA [SU(3), O(6), and U(5)], simple analytic formulas can be obtained by group-theoretical algebra and written in the general form [6]

$$B(E2{:}2_1^+\rightarrow 0_1^+)=f(N)^2(e_\pi N_\pi+e_\nu N_\nu)^2 \ , \tag{7}$$

where

$$f(N)^2=\begin{cases}\dfrac{1}{N} & \text{for U(5)} \ ,\\ \dfrac{2N+3}{5N} & \text{for SU(3)} \ ,\\ \dfrac{N+4}{5N} & \text{for O(6)} \ ,\end{cases} \tag{8}$$

and $N=N_\pi+N_\nu$. Ginocchio and Van Isacker [6] have pointed out that, even though a nucleus may be close to the vibrational [U(5)] limit, the appropriate $f(N)$ function can be quite different from $1/N$. They proposed [6] a different relation, derived by expanding $f(N)$ in leading-order perturbation theory near the U(5) limit:

$$f(N)^2=\frac{1}{N}\left[1-\frac{\kappa(N-1)}{\varepsilon}\right]^2 . \tag{9}$$

The O(6) and SU(3) equations are more stable with respect to deviations from the exact symmetry.

Most "real" nuclei do not follow any one of the above limiting symmetries. However, many nuclei can be considered as transitional between two of the three symmetries. One can therefore look upon these nuclei as being "located" at some point along one of the three sides of the "IBA triangle" [7] (see Fig. 1). Many nuclei (e.g., most of the rare-earth nuclei) are intermediate between O(6) and SU(3): That is, they can be well described by the Hamiltonian of Eq. (4) with $\varepsilon=0$. For these nuclei the following approximate analytic formula was obtained in Ref. [8]:

$$B(E2{:}2_1^+\rightarrow 0_1^+) \approx 0.25(1-0.1\chi)^2\left[\frac{N+1}{N}\right]^2(e_\pi N_\pi+e_\nu N_\nu)^2 \ , \tag{10}$$

where χ is related to χ_π and χ_ν of Eq. (5) and is defined by

$$\chi=(\chi_\pi N_\pi+\chi_\nu N_\nu)/N \ . \tag{11}$$

Equation (10) was found [8] to reproduce numerical IBA calculations within about 15% for deformed nuclei.

Of course, many nuclei require a still more general Hamiltonian. To deal with such cases, we need an analytic formula for $B(E2{:}2_1^+\rightarrow 0_1^+)$ values which is valid for all three sides of the triangle and its interior. Such an expression has recently been developed and discussed in detail in Ref. [9]. Two parameters are needed in order to scan the triangle. These are χ defined above and ξ, defined by [9]

$$\xi=\frac{\eta}{\eta+1} \ , \tag{12}$$

with

$$\eta=\frac{4(N-1)\kappa}{\varepsilon} \ .$$

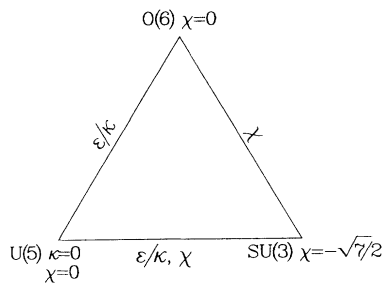

FIG. 1. Symmetry triangle of the IBA. The parameters giving each symmetry and determining position along the transition legs are given.

The values of χ and ξ for the specific symmetries are

$$\chi=0,\ \text{O(6)};\quad -\sqrt{7}/2,\ \text{SU(3)}\ ; \tag{13}$$

$$\xi=0\ ,\ \text{U(5)};\quad 1,\ \text{SU(3) and O(6)}\ . \tag{14}$$

In terms of these parameters, it was shown in Ref. [9] that a good analytic approximation to detailed numerical diagonalizations is

$$B(E2{:}2_1^+\rightarrow 0_1^+)\approx 0.25[1+0.2(1+\tfrac{4}{7}\chi^2)g(\xi)(N-1)] \times\frac{1}{N}(e_\pi N_\pi+e_\nu N_\nu)^2\ , \tag{15}$$

with

$$g(\xi)=\frac{1}{1+2(1/\xi-1)^2}\ . \tag{16}$$

The free parameters in this equation can be estimated using expressions based on a microscopic shell-model description. These expressions are described in some detail in Ref. [9].

To summarize, we have now six different analytic relations for $B(E2{:}2_1^+\rightarrow 0_1^+)$ transition probabilities: the three equations for the limiting symmetries [Eqs. (8)], the "perturbed U(5)" formula [Eq. (9)], Eq. (10) for deformed nuclei, and Eq. (15), which spans the "IBA triangle." For convenience, we will refer from now on to Eq. (10) as to the "analytic" formula and to Eq. (15) as the "triangular" formula. All the equations have the form

$$B(E2{:}2_1^+\rightarrow 0_1^+)=f(N)^2(e_\pi N_\pi+e_\nu N_\nu)^2\ , \tag{17}$$

where $f(N)$ is a generalization of the functions with the same name in Eqs. (8) and may also depend on the parameters ε,κ,χ. For the "perturbed U(5)" formula [Eq. (9)], $f(N)$ depends on the ratio κ/ε. This ratio can be determined by using a phenomenological approach as described in Ref. [10]. For the "analytic" formula [Eq. (10)], $f(N)$ depends on χ. However, it is a rather weak functional dependence, and so the results are hardly sensitive at all to the particular χ value chosen for the bulk of deformed nuclei. For most deformed nuclei, a reasonable choice for χ is -0.4, and this is the value we used in this work. Finally, for the "triangular" formula [Eq. (15)], $f(N)$ depends on χ,ξ. These parameters can be calculated using a microscopic shell-model approach as described in Ref. [9]. We take the parameters of Ref. [9], and hence, in this case, in fact there are no free parameters.

Equation (17) can be rewritten as

$$\frac{1}{N_\nu}\left[\frac{1}{f(N)^2}B(E2{:}2_1^+\rightarrow 0_1^+)\right]^{1/2}=\left[e_\nu+e_\pi\frac{N_\pi}{N_\nu}\right]\ . \tag{18}$$

We now define

$$T\equiv\frac{1}{N_\nu}\left[\frac{1}{f(N)^2}B(E2{:}2_1^+\rightarrow 0_1^+)\right]^{1/2}\ . \tag{19}$$

From Eqs. (18) and (19), it is clear that T is a linear function in N_π/N_ν. T can be calculated using the experimental $B(E2)$ and one of the six expressions for $f(N)$. If this is done for several neighboring nuclei and if we assume that the effective boson charges are approximately the same for these nuclei, then e_π,e_ν can be extracted directly by making a linear fit of T against N_π/N_ν. This general method for determining e_π,e_ν was used before by several authors [11–16] for a few isotopic and isotonic chains. In general, our values are in agreement with their results. However, there is an important difference between our work and all the previous publications. In addition to the relations applicable to the limiting symmetries which were used in the other works, we also use approximate analytic formulas which were shown [8,9] to provide a better description of transition probabilities in real nuclei, which, nearly always, deviate from the exact dynamical symmetries. In this way we obtained a consistent set of e_π,e_ν values for chains of isotopes with $42\leq Z\leq 96$, which reproduce reasonably well $B(E2)$ experimental data when introduced in the appropriate analytic relation. Other approaches to this problem are possible. For example, Hamilton [15] has deduced e_π values by making fits to isotopic chains and e_ν values from isotonic chains. Although this procedure is valid in principle, the deduced effective charges for a specific isotope do not always reproduce correctly the experimental $B(E2)$ value, because they were extracted from different fits to different sets of nuclei. In an entirely different approach, Barfield and Lieb [17] and Giannatiempo *et al.* [18] have extracted charges for individual isotopes from several experimental $E2$ transition probabilities in each nucleus and by calculating matrix elements of the quadrupole operators with an IBA-2 code. This procedure differs from ours in that it provides effective charges for each isotope. However, it leads to some ambiguity because it gives two sets of solutions and thus requires more experimental data in order to distinguish between them. Moreover, by using some less collective transitions in their fits, their results are more likely to be affected by inaccuracies in details of the treatments of various intrinsic excitations. A more important point is that the values and even the physical meaning of e_π and e_ν are intrinsically connected to their method of extraction, and detailed comparisons of different extracted effective charges should be made with this in mind. We return to this point in Sec. III D.

The main issue in using the method we described above for the extraction of e_π,e_ν by fits of T vs N_π/N_ν is to decide which relation to use for each set of nuclei. This decision is sometimes a little ambiguous because, as we mentioned before, "real" nuclei do not follow well-defined rules and simple models. In order to circumvent this difficulty, we used at least two or three relations for each fit. For example, we used the SU(3), the "analytic" and the "triangular" formulas to fit deformed nuclei. For vibrational nuclei we usually used the "pure" U(5) and "perturbed" U(5) equations. In all cases the "adopted" effective charges were arithmetic averages of the values from the various fits. We attached "error bars" to them, which reflect the differences in the values obtained with the different formulas used.

Another problem arises when one of the isotopes involved in the fit has a magic number of neutrons. In that

case $N_\nu=0$ and N_π/N_ν as well as T are not determined. For these fits we rewrite Eqs. (18) and (19) in terms of N_ν/N_π instead of N_π/N_ν and proceed as before. Finally, it may happen that a chain of isotopes spans a transition region such that different subsets of isotopes have significantly different structure. In such cases the chain must be split into parts and the appropriate analytic formulas used for each part.

III. RESULTS

A. Examples of individual fits

We used about 120 $B(E2{:}2_1^+\rightarrow 0_1^+)$ values for nuclei with $A>90$. We divided them into 25 groups, with about 3–8 isotopes in each group. Special care was taken to include in one group only nuclei having similar structure. Generally, an entire isotopic chain can be used in this way, but as noted above, there are isolated cases where a vibrational-rotational transition occurs within one isotopic chain (e.g., Mo and Ba). In these cases we formed two groups for the same element and made fits with different formulas.

We now present a few examples of the fits and the extracted e_π and e_ν values. In Fig. 2 we present the fits for the $^{104-110}$Pd and $^{154-160}$Gd isotopes, using three different algebraic relations in each case to calculate the value of T. We see that the resulting e_π,e_ν are not very different, thereby lending confidence to the extraction of an average set with reasonably small uncertainties. The "adopted" values in this case are $e_\pi=0.15(2)$ e b, $e_\nu=0.08(1)$ e b for Pd and $e_\pi=0.18(3)$ e b, $e_\nu=0.09(1)$ e b for Gd. The error bars include the variations due to the different relations used.

It is interesting to compare our results for the Pd isotopes with those of Saha *et al.* [3], who used $\pi^\pm$ scattering amplitudes to extract effective charges $e_p=1.13e$, $e_n=0.49e$, for the same Pd isotopes, $^{104-110}$Pd. These quantities are related to e_π,e_ν by

$$e_\pi=\alpha_p e_p,\quad e_\nu=\alpha_n e_n\ , \tag{20}$$

where α_p,α_n are expectation values of the quadrupole operators, which were calculated in a generalized seniority scheme, yielding $\alpha_p=15.2$ fm^2, $\alpha_n=16.4$ fm^2. Using Eq. (20), we obtain $e_\pi=0.17$ e b, $e_\nu=0.08$ e b, in excellent agreement with our results. Moreover, Saha *et al.* [3] obtained essentially the same e_p,e_n for all isotopes considered, thus supporting our assumption of constant

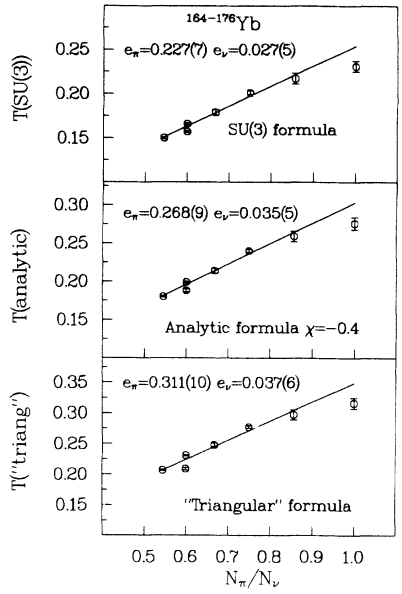

FIG. 3. Fits of $B(E2)$ experimental data for the $^{164-176}$Yb isotopes (see caption to Fig. 2).

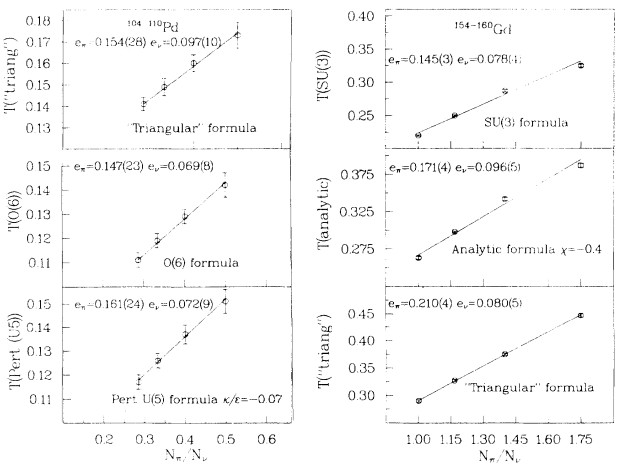

FIG. 2. Left: fits of $B(E2)$ experimental data for the $^{154-160}$Gd isotopes, using three different relations for T: the SU(3) formula [Eq. (8)], the analytic formula [Eq. (10)], and the "triangular" formula [Eq. (15)]. See Eq. (19) for the definition of T. Error bars on the experimental points are given: They are often smaller than the point size. Right: similar for $^{104-111}$Pd.

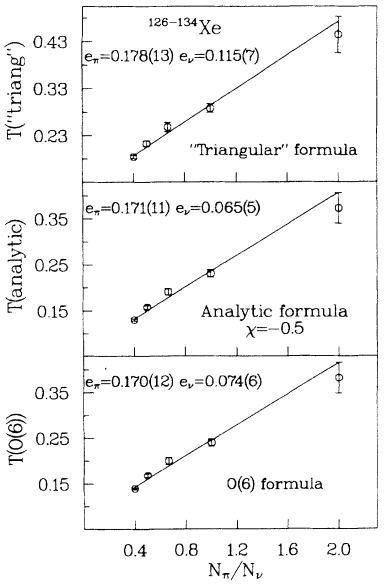

FIG. 4. Fits of $B(E2)$ experimental data for the $^{126-134}$Xe isotopes (see caption to Fig. 2).

effective charges for isotopes of a given element.

In Fig. 3 we present the results for the $^{164-176}$Yb isotopes, where a small value of e_ν was obtained, and in Fig. 4 the fits for the $^{126-134}$Xe isotopes are given.

B. Effective charges in the $A=150$ region

The neutron-rich nuclei in the $A=150$ region are known to exhibit a pronounced transition from vibrational to deformed/rotational shape. This onset of deformation has been interpreted [19] as being due to the $1h_{9/2}$-$1h_{11/2}$ p-n interaction, which becomes increasingly significant as neutrons are added beyond $N=88$. This interaction also causes the $Z=64$ subshell, which is a "good" subshell for nuclei with $N\leq 88$, to practically disappear for $N\geq 90$.

For some vibrational Ba, Ce, and Nd isotopes, Hamilton, Irbäck, and Elliott [11] have reported anomalous effective charges $e_\nu=0.24\ e$ b, $e_\pi=0.12\ e$ b, with $e_\nu > e_\pi$. They obtained the results from fitting $B(E2)$ transition probabilities and using the U(5) relation [Eq. (8)]. The validity of this surprising result was questioned by Ginocchio and Van Isacker [6], who claimed that the "pure" U(5) relation cannot be used reliably because it is unstable to small deviations from the U(5) symmetry.

In this work, despite attempts to avoid this seemingly anomalous result, we find clear evidence supporting enhanced e_ν/e_π values in the vibrational ^{138,142,144}Ba, ^{140,142,146}Ce, $^{142-146}$Nd, and ^{144,148,150}Sm isotopes. In Fig. 5 we present the fits for the three Ba isotopes. We see that, although the absolute values of e_π and e_ν are not the same for the three fits, the ratio of e_ν/e_π is considerably larger than 1 even when the perturbed U(5) [Eq. (9)] or the "triangular" [Eq. (15)] formulas are used. The ratio is in the range 1.5–2.0, in approximate agreement with the value of 2.0 reported in Ref. [11]. For the Ce, Nd, and Sm isotopes, the analysis is somewhat more complicated because of the $Z=64$ subshell, which is presumably still active in the isotopes considered. Under this assumption the valence numbers of proton bosons (N_π) are 3, 2, and 1 for the Ce, Nd, and Sm isotopes, respectively. In Fig. 6 we present the results for the Sm isotopes. The fits in Figs. 6(a) and 6(b) were obtained assuming $N_\pi=1$ for all three isotopes. We see that the ratio e_ν/e_π in

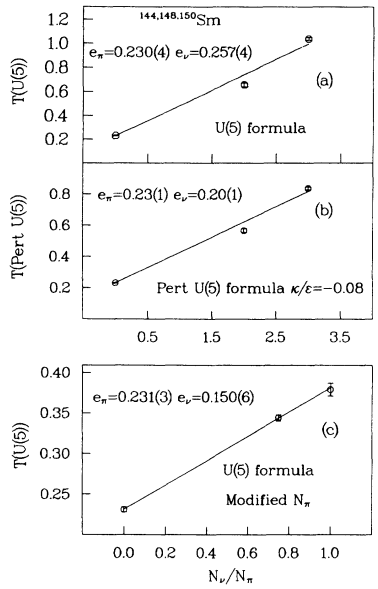

FIG. 6. Fits of $B(E2)$ experimental data for the ^{144,148,150}Sm isotopes (see caption to Fig. 2). Fit (c) is explained in the text.

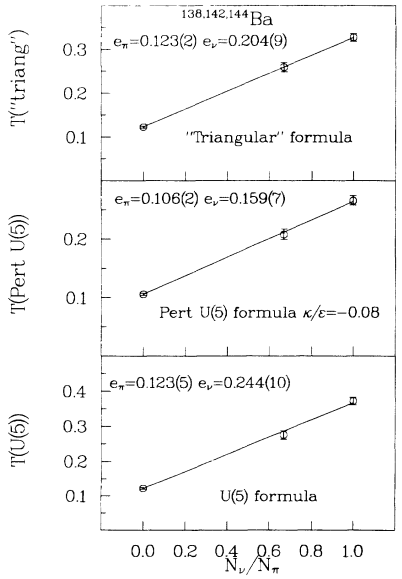

FIG. 5. Fits of $B(E2)$ experimental data for the ^{138,142,144}Ba isotopes using the "pure" U(5) formula [Eq. (8)], the U(5) perturbed formula [Eq. (9)], and the "triangular" formula [Eq. (15)].

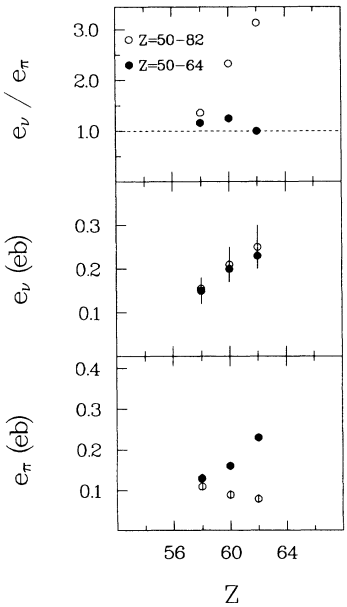

FIG. 7. Effective charges e_π, e_ν and the ratios e_ν/e_π for the ^{140,142,146}Ce, $^{142-146}$Nd, and the ^{144,148,150}Sm isotopes. The dots indicate the results obtained using the $Z=50$–64 shell. The circles are the results from fits assuming the full $Z=50$–82 shell.

these two fits is 0.9 and 1.1, respectively [i.e., still considerably enhanced with respect to the expected (and typically found) values in the range 0.3–0.5]. The fit of Fig. 6(c) will be discussed later.

In Fig. 7 we present the values of e_π, e_ν, and e_ν/e_π obtained for the Ce, Nd, and Sm isotopes. The dots indicate the results obtained assuming that the $Z=64$ subshell is active, while the circles are from fits using the full 50–82 shell (i.e., using $N_\pi=4$, 5, and 6 for Ce, Nd, and Sm, respectively). The ratio e_ν/e_π is larger than 1.0 in all cases. It should be noted that the strong increase of e_π from about 0.11 in Ce to about 0.23 in Sm, where the $Z=50-64$ shell is used, is due to the fact that N_π decreases from 3 (for Ce) to 1 (for Sm), and since the transition probability contains the product $e_\pi N_\pi$ [see, e.g., Eq. (18)], a smaller N_π in effect requires a larger e_π to produce the same $B(E2)$ value.

The enhanced e_ν/e_π ratio in the $A=150$ region can be qualitatively seen also by directly inspecting the experimental $B(E2)$ data. In Fig. 8 we present the $B(E2)$ values for isotopes in this region (from Ref. [9]; data are from Ref. [4]). We see that for the Ba, Ce, Nd, and Sm isotopes, the N dependence of the $B(E2)$ values for $N=82-88$ is much stronger than the Z dependence. This larger sensitivity to changes in N_ν than N_π implies the need for a larger multiplier of N_ν than of N_π in the expression for $B(E2)$ values.

To summarize, the above arguments show that the large e_ν/e_π values in the $A=150$ region are not an artifact of the way the data is analyzed and are not due to the "instability" of the U(5) formula, but rather are a real effect exhibited by the nuclei in this region.

C. Systematics of e_π, e_ν across the periodic table

In Fig. 9 we present the e_π, e_ν, and e_ν/e_π obtained from the analysis of the 120 $B(E2)$ experimental values considered in this work. Several features arise from examining this figure.

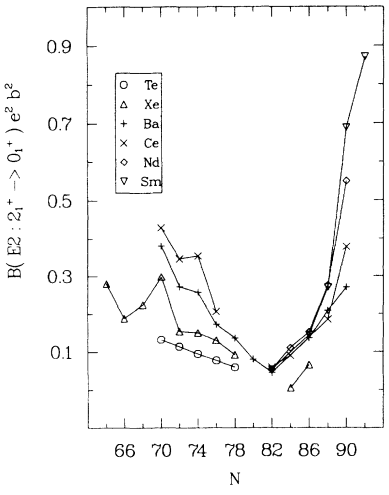

FIG. 8. Experimental $B(E2{:}2_1^+ \rightarrow 0_1^+)$ values for Te, Xe, Ba, Ce, Nd, and Sm isotopes (from Ref. [9]; data are from Ref. [4]).

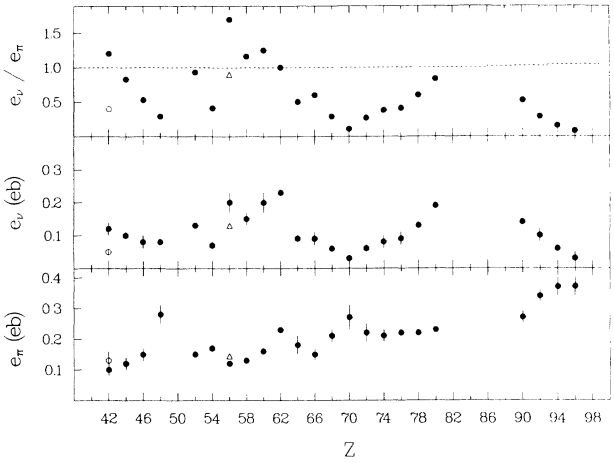

FIG. 9. Systematics of e_π, e_ν as a function of Z. The open circle indicates the results for the deformed $^{102-108}$Mo isotopes, and the open triangle gives the fitted value for the deformed, $N<82$, $^{128-134}$Ba isotopes. The error bars show the range of variation due to the various formulas used.

(a) The values of e_π increase almost monotonically with Z from about 0.12 at $Z=42$ to almost 0.4 at $Z=96$.

(b) The values of e_ν show pronounced and systematic variations with respect to Z. Very large (0.15–0.2 e b) e_ν's are observed at $Z=56-62$; then they decrease to values as low as about 0.03 e b at $Z=70$ and then increase again toward $Z=82$. Then we see again a decrease in e_ν in the actinides.

(c) The ratios e_ν/e_π are close to and sometimes above 1.0 in three regions: $Z=42-44$, $Z=56-62$, and $Z\sim82$. For most deformed nuclei, the ratio e_ν/e_π is between 0.3 and 0.5, as expected from the prediction of Bohr and Mottelson [1] [Eq. (3)]. A significant drop in this ratio nearly to zero is observed around $Z=70$ and then again at $Z=96$.

The appearance of several regions, where $e_\nu \gtrsim e_\pi$, and of others, near midshell, where e_ν is very small, leads to a recurring *undulating* pattern in e_ν and e_ν/e_π. The regularity suggests a simple underlying explanation related to general features of shell structure and residual interactions.

D. Fits to isotonic and isobosonic chains of nuclei

In the present work, we are mainly concerned with effective charges pertaining to isotopic chains. It is important to recognize that the boson effective charges e_π and e_ν, as extracted with the approach discussed here, are not defined with respect to a specific nucleus. Their extraction explicitly entails a *sequence* of nuclei, and they reflect the *changes* in $B(E2)$ values across such a sequence. There is, indeed, the explicit assumption that e_π and e_ν are constant across such sequences. Both the absolute values and the physical interpretation of the

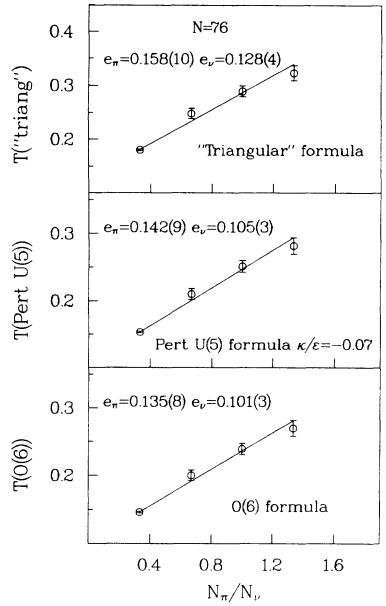

FIG. 10. Fits of $B(E2)$ experimental data for the $N=76$ isotones (see caption to Fig. 2).

present e_π, e_ν values may differ from those extracted, for example, from several $E2$ transitions in a single nucleus.

In view of this, it is interesting to extract e_π and e_ν values for other sequences of nuclei such as isotonic, "isobosonic" (which can either be isobaric or $\Delta A=4$ sequences), or even iso-N_pN_n series. This is an extensive program which will be the subject of a further investigation. Here we illustrate the idea with two examples. In Figs. 10 and 11 we show fits for the isotonic chain $N=76$ and for the "isobosonic" $\Delta A=4$ chain $N_t=15$ (i.e., $N_\pi+N_\nu=15$). In each case e_π and e_ν are taken as constants across the particular sequence studied. It is expected that a systematic analysis of all possible fits of this kind, together with the isotopic fits presented in detail in this work, will provide further information on the dependence of the effective charges on N and Z and on how e_π and e_ν values in a given region depend on the sequence of nuclei inspected.

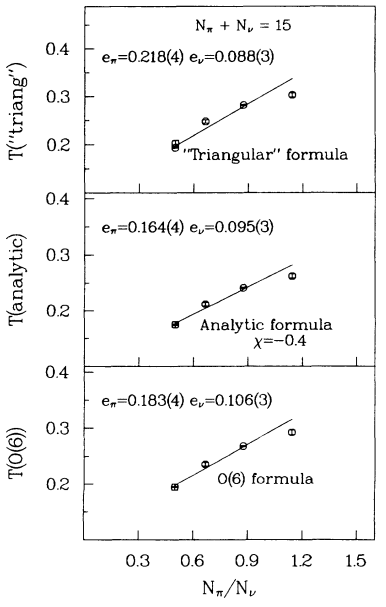

FIG. 11. Fits of $B(E2)$ experimental data for the isobosonic nuclei with $N_t=N_\pi+N_\nu=15$ in the rare-earth nuclei near $A=160$ (see caption to Fig. 2).

IV. DISCUSSION

We have alluded to an interpretation of effective charges in valence models in terms of derivatives of matrix elements with N_π and N_ν. It is easy to see the rationale for this. All the analytic expressions for $B(E2)$ values have the form of Eq. (17). Hence, defining $M(E2)\equiv\sqrt{B(E2)}$, we can write

$$M(E2:2_1^+\rightarrow 0_1^+)=f(N)(e_\pi N_\pi+e_\nu N_\nu)\ . \tag{21}$$

The essential point in the discussion to follow is that $f(N)$ is *slowly* varying with N. This is particularly true for the SU(3) and O(6) limiting symmetries where a unit change in N typically changes $(e_\pi N_\pi+e_\nu N_\nu)$ by about 20% while $f(N)$ changes only by 1–3%. It is also true for the other analytic relations, though somewhat less so for U(5)-like nuclei. We will return to this more quantitatively just below. Suffice it to summarize by concluding that, at least for a semiquantitative analysis, we can treat $f(N)$ as constant. If we then differentiate $M(E2)$ with respect to N_π and N_ν, we get

$$\begin{aligned}\frac{\partial M}{\partial N_\nu}&=\sim f(N)e_\nu\sim e_\nu\ ,\\ \frac{\partial M}{\partial N_\pi}&=\sim f(N)e_\pi\sim e_\pi\ .\end{aligned} \tag{22}$$

Hence e_π and e_ν are approximately proportional to the derivatives of $M(E2)$ with N_π and N_ν, respectively, and therefore serve as measures of the rate of change of the nuclear collectivity in the ground-state region with changing proton and neutron numbers across the series of nuclei used in the linear fits to extract the effective charges. Such a simple, physically intuitive, role for effective boson charges is peculiar to valence models, where N, N_π, and N_ν explicitly enter the formalism and confer on these quantities a high interest since they can now be exploited to study separately the respective roles of protons and neutrons in the evolution of collectivity and, as we shall see, to study some subtle effects in the p-n interaction.

Given the importance of the concept embodied in Eqs. (22), it is worthwhile being more quantitative. It is easy to use Eqs. (8) to write explicitly

$$\frac{\partial M(E2)}{\partial N_\pi}=\tfrac{1}{2}f(N)\times\begin{cases}\left[2-\dfrac{3N_\pi}{N(2N+3)}\right]e_\pi-\dfrac{3N_\nu}{N(2N+3)}e_\nu, & \mathrm{SU}(3)\\ \left[2-\dfrac{4N_\pi}{N(N+4)}\right]e_\pi-\dfrac{4N_\nu}{N(N+4)}e_\nu, & \mathrm{O}(6)\\ \left[2-\dfrac{N_\pi}{N}\right]e_\pi-\dfrac{N_\nu}{N}e_\nu, & \mathrm{U}(5)\ .\end{cases}\tag{23}$$

[Similar equations are, of course, obtained for $\partial M(E2)/\partial N_\nu$.] The validity of our assertion in Eqs. (22) is determined by the relative sizes of the coefficients of e_π and e_ν, as well as by the rate of change of the coefficient of e_π with N and N_π. To study this we write $M(E2)=\frac{1}{2}f(N)(Ae_\pi-Be_\pi)$. Simple manipulation then gives

$$A/B=\begin{cases}\dfrac{4N^2+3N}{3N_\nu}+1, & \mathrm{SU}(3)\\ \dfrac{N^2+2N}{2N_\nu}+1, & \mathrm{O}(6)\\ \dfrac{N}{N_\nu}+1, & \mathrm{U}(5)\ .\end{cases}\tag{24}$$

The smallest (worst) ratio A/B is obtained for the largest N_ν, namely, $N_\nu=N$, which gives

$$A/B\geq\begin{cases}\dfrac{4N^2+3N}{3N}+1=\dfrac{4}{3}N+2, & \mathrm{SU}(3)\\ \dfrac{N^2+2N}{2N}+1=\dfrac{N}{2}+2, & \mathrm{O}(6)\\ \dfrac{N}{N}+1=2, & \mathrm{U}(5)\ .\end{cases}\tag{25}$$

For *all* three limits, therefore, A is the leading-order term. For SU(3) and O(6), where, usually, $N>6$, $A/B\gg 1$ and even in U(5) $A/B>2$.

Finally, we note that for the SU(3) and O(6) expressions [as well, of course, as the intermediate expression Eq. (10)], the second term in A and the coefficient B go to zero in the large-N limit so that Eqs. (22) are recovered exactly.

Thus, in all cases, e_π and e_ν are, to good approximation, proportional to the rates of change of $M(E2)$ with N_π and N_ν, respectively, and, hence [since $M(E2)$ is a standard measure of collectivity], e_π and e_ν are proportional to the growth of collectivity as a function of N_π and N_ν across a series of nuclei.

This simple point confers on the effective charges a physical significance they lack in many other approaches. We now exploit this to interpret the e_ν systematics, especially in the regions of very large e_ν/e_π ratios near or exceeding unity. We will interpret the systematic variations of e_ν vs Z qualitatively as being due to two major factors, both originating in the *p-n* interaction: (a) polarization of the proton single-particle structure as a function of neutron number; this applies in both the $A\sim 100$ and 150 regions (and possibly in the actinides); and (b) saturation of the *p-n* interaction strength near midshell regions.

We first focus on the large e_ν/e_π values in several regions of Fig. 9. From our interpretation in terms of derivatives, it will be seen that, far from being suspect or incomprehensible, the large e_ν values found by Hamilton, Irbäck, and Elliot [11] for $A\sim 150$, and appearing in three regions in Fig. 9, are in fact easily understandable and in accord with the microscopic evolution of collectivity in these regions.

The question is, what is the meaning of enhanced e_ν and e_ν/e_π values? At the most superficial level they simply mean that the addition of neutrons is more effective in generating collectivity than protons. This, for example, is apparent in our earlier discussion of Fig. 8. The deeper issue is why this is so. Reflection on the structural evolution of the $A=100$ and 150 regions supplies an answer. The valence neutrons here play a *dual* role. The first is the usual one of contributing to the buildup of (primarily *p-n*) valence space (primarily quadrupole) interactions (that is, to increasing N_pN_n). The second is that of polarizing the protons. In particular, in both regions, neutrons fill critical states with large overlaps with the proton j shells $1g_{9/2}$ ($A\sim 100$) and $1h_{11/2}$ ($A\sim 150$). The *monopole p-n* interaction then acts to *lower* these proton single-particle energies [20], eradicating the well-known subshell gaps at $Z=38$ (or 40) and 64 and thereby contributing to an effective increase in the number of valence protons as each neutron is added. Since N_π is constant for a series of isotopes, in the analytic expressions for $B(E2{:}2_1^+\rightarrow 0_1^+)$, this polarization effect appears as an enhanced efficiency of the neutrons via a larger e_ν.

It is actually possible quantitatively to test this scenario. In the calculation of e_π, e_ν for the Ba, Ce, Nd, and Sm isotopes, we assumed that the $Z=64$ subshell is active [19], since we considered only $82\leq N\leq 88$ isotopes. This assumption is certainly very crude. One expects the "disappearance" of the subshell to be gradual. In fact, an analysis of g-factor and $B(E2)$ data for nuclei in this region has indeed shown that a gradual dissipation of the subshell takes place [12] for $N=84$–90. This means that in a given isotopic chain, e.g., ^{144,148,150}Sm, the "effective" number of valence protons increases as the number of neutrons increases. While for ^{144}Sm we expect $N_\pi=1$ (i.e., the subshell is active), in ^{152,154}Sm the subshell is no longer active and therefore we have $N_\pi=6$ for these isotopes. For ^{148,150}Sm we therefore expect values of N_π intermediate between 1 and 6. If we include this "dissipation" effect in the $B(E2)$ fits, we should obtain a lower e_ν because the effect of valence neutrons on the effective valence proton number is now made explicit in the choice

of N_π values. Such a test is illustrated in Fig. 6(c), where we present the linear fit in which we used $N_\pi = 1,2,4$ for ^{144,148,150}Sm, respectively. We see that while e_π does not change with respect to the fits in Figs. 6(a) and 6(b), where $N_\pi = 1$ was assumed for all the isotopes, e_ν is considerably smaller. In fact, the ratio e_ν/e_π for the fit in Fig. 6(c) is 0.65, i.e., much closer to "normal" values.

Therefore the large e_ν/e_π values in the $Z = 56-62$ region are a manifestation of the "dissipation" of the $Z = 64$ subshell. The fact that we get a large e_ν/e_π also for the Ba isotopes, which, with $Z = 56$, is not affected by the $Z = 64$ subshell, implies that other effects may also contribute to the enhanced values of e_ν and, therefore, of e_ν/e_π. This is deserving of further study.

The enhanced e_ν and e_ν/e_π values in the $A \sim 100$ region point to the same interpretation there. In both the $A = 100$ and 150 regions, the cessation of this dual role for the neutrons, once deformation has set in, is nicely illustrated in Fig. 9 by the second points (open symbols) for the rotational Mo and Ba isotopes where more "normal" e_ν values are obtained after the phase transition.

It is interesting to note that large e_ν and e_ν/e_π values also occur in the preactinides. Indeed, e_ν/e_π may again exceed unity, although the data just above $Z = 82$ are lacking. This enhancement is also worth studying since no subshell effects, such as are those for the $A \sim 100$ and 150 region, are known here. Our results point to the possible existence of a heretofore undetected subshell effect in the trans-Pb region. This speculation is interesting in light of an anomaly previously noted in N_pN_n plots. Using normal shell closures, Cizewski and Dieperink [21] found that N_pN_n plots for the actinides are noticeably steeper than for *any* other region in medium and heavy nuclei. If, however, a subshell and its dissipation were invoked, the N_pN_n curves would flatten out, more in line with those from other regions. The conjunction of these hints of such an effect both from the neutron effective charges and, in retrospect, from N_pN_n plots suggests that further study (and data) in this region would be worthwhile.

It should be pointed out that the rise in e_ν just before the Pb region, again showing enhanced structural sensitivity to the number of neutrons, has not yet been amenable to a similar interpretation. Further study of these high e_ν and e_ν/e_π values should prove interesting.

We now turn our attention to very small values of e_ν and e_ν/e_π around $Z = 70$ and 96. We recall that e_ν and e_π are approximately the derivatives of the $E2$ $2_1^+ \rightarrow 0_1^+$ matrix element with respect to N_ν and N_π, respectively. The $E2$ matrix element depends strongly on the nuclear deformation and is of course related to the quadrupole moment of the nucleus. We therefore expect this matrix element to behave approximately as the function S_{pn}:

$$S_{pn} = \sum_{i,j} a_i Q_{p_i} Q_{n_j} , \tag{26}$$

where the sum is over all relevant Nilsson orbitals and Q_{p_i} (Q_{n_j}) is the quadrupole moment of a proton (neutron) in orbit $i(j)$. S_{pn} was defined and discussed in Ref. [22] and gives a good approximation to the quadrupole p-n interaction strength. In particular, a microscopic calculation shows [22] that S_{pn} saturates when the middle of the 82–126 neutron shell is approached. This saturation effect is due to the smaller overlap of proton and neutron wave functions when near midshell orbits are filling, since orbits with many different angular orientations to the equatorial plane are then occupied, with varying mutual overlaps, compared with the situation early in a shell when all filled orbits are highly aligned along the equatorial plane. It was shown in Ref. [22] that S_{pn} can be related to $B(E2{:}2_1^+ \rightarrow 0_1^+)$ values and that the saturation in S_{pn} ($\partial S_{pn}/\partial N_n \sim 0$) corresponds to a saturation in $B(E2)$ values. Thus the very small e_ν values, near midshell in both the rare earths and actinides, reflect the almost negligible contribution of midshell neutrons to any increase in collectivity.

We noted earlier that the empirical e_ν and e_ν/e_π values exhibit an undulating pattern. This regular behavior can now be understood in terms of the above analysis. In shape/phase transitional regions, recurring regularly at the beginning and end of major shells, valence neutrons may have an amplified effect on the development of collectivity, helping to polarize the proton shell structure and, in particular, to eradicate proton shell closures. This amplification is reflected in rather large values of e_ν and e_ν/e_π. In contrast, near the neutron midshell, where the saturation of collectivity occurs, e_ν is very small. These two effects, repeated for each shell, account for the recurring undulations in e_ν and e_ν/e_π.

We have offered interpretations of a number of the features of e_ν and e_ν/e_π in Fig. 9, in particular of the mechanisms that can account for some of the maxima in e_ν and its midshell minima. There are, however, two features of the empirical systematics worth further elucidation, namely, the large values of e_ν just before the $Z = 82$ shell closure in the Os-Pt and Hg isotopes and the nearly linear increase in e_π across medium and heavy nuclei. The lack of pronounced oscillations in e_π is probably reasonable since the respective filling of neutron and proton shells near the valley of stability does not lead to situations in which neutron shell or subshell gaps are eradicated by the filling of particular proton orbitals. However, the secular increase of e_π merits further microscopic interpretation.

Finally, we note that the boson effective charges are closely related to the concept of F-spin symmetry [23]. In a given nucleus, the maximum value of F is $(N_\pi + N_\nu)/4$. Maximum F spin corresponds to total proton-neutron symmetry and is the limit in which the IBA-1 coincides with predictions of the IBA-2. It is generally expected [24] that the F spin is a good quantum number for the low-lying states, which are nearly pure $F_{\max}$ states, although some calculations have invoked [25] substantial F-spin mixing. The best known $F < F_{\max}$ states are the isovector $M1$ "scissors" mode 1^+ levels [26] occurring near 3 MeV in many medium mass and heavy nuclei. It has been discussed [15,27] that the quantity $(e_\pi - e_\nu)$ is important in elucidating the amount of F-spin mixing. Since the issue of F-spin purity is an active area of study, it is interesting to show explicitly the

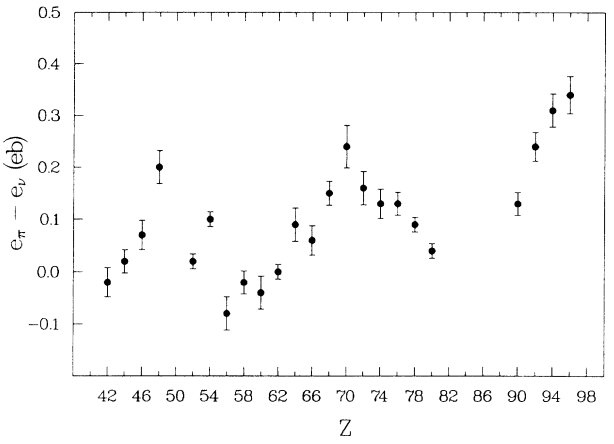

FIG. 12. Values of e_π-e_ν extracted from the solid points in Fig. 9.

empirical e_π-e_ν values from our study. These are plotted in Fig. 12. The most notable feature is, again, an undulation, mirroring the undulations in e_π/e_ν, in which (e_π-e_ν) maximizes near midshell where the saturation in collectivity leads to very small values of e_ν.

V. CONCLUSIONS

Effective proton and neutron boson charges e_π and e_ν were extracted from $B(E2{:}2_1^+ \rightarrow 0_1^+)$ values in even-even isotopic chains from $Z=42$ to the actinides using analytic formulas based on the IBA. The effective charge of the proton was found to behave quite smoothly as a function of Z. The rather smooth behavior of e_π may be amenable to interpretation with the schematic model of Bohr and Mottelson [1]. According to this model, e_π has a constant term [see Eq. (1)], and therefore its Z and A dependence is expected to be weaker than that of e_ν. In contrast, e_ν exhibits quite dramatic variations, from values as large as 0.2 e b around $Z=56$, down to 0.03 e b at $Z=70$ and in the actinides. Indeed, e_ν and e_ν/e_π seem to oscillate rather regularly across each shell, peaking close to magic numbers and minimizing near midshell. We have shown that effective charges in valence models play a fundamentally different role than in traditional approaches, namely, as (proportional to) the derivatives of "collectivity" [measured by $M(E2{:}2_1^+ \rightarrow 0_1^+)$ values] with changes in the valence proton or neutron number. We stress here that these effective charges are defined only by references to the specific isotopic chains for which they were extracted. Different effective charges will, in general, be obtained for isotonic or other sequences, even involving the same nuclei, because the growth of collectivity may not be isotropic in the N-Z plane, but can depend on the direction in which a series of nuclei cuts across this plane. In complex regions of rapid structural change, e_π and e_ν may be very dependent on the nuclei inspected, whereas in regions of stable structure such as in the Pd region, e_π and e_ν seem to be less sensitive to the specific chain of nuclei. The thorough study of various sequences will allow one to map the proton and neutron dependence of collectivity in arbitrary directions in the N-Z plane; this is the subject of an on-going study and is well beyond the scope of the present work.

An analysis in terms of the "derivative" concept allows one to disentangle the respective roles of protons and neutrons in the growth of collectivity. In analyzing the enhanced e_ν and e_ν/e_π values in several regions of the nuclear chart, we have shown that these variations are due mainly (but not only) to the p-n interaction dependence on nucleon number. In the $Z=56$ region, the $\pi h_{9/2}$-$\nu h_{11/2}$ interaction causes the $Z=64$ shell to "disappear." This in turn is reflected in enhanced e_ν values and points to a dual role for neutrons in this region: In addition to contributing to the buildup of valence nucleons (and $N_p N_n$), they also alter the proton space, contributing to an effective increase in valence proton number. A similar interpretation applies in the $A=100$ region and, perhaps, points to an analogous, heretofore undetected, modulation of proton shell structure in the preactinide transitional region as well. As more nucleons are added, the p-n interaction saturates and e_ν becomes very small, reflecting the fact that $M(E2{:}2_1^+ \rightarrow 0_1^+)$ values become almost constant near midshell, where additional neutrons, in orbits with small quadrupole moments and poor overlap with many of the filled proton orbits, contribute little to further enhancement of collectivity.

ACKNOWLEDGMENTS

We are grateful to J. Ginocchio, A. Leviatan, P. von Brentano, and N. V. Zamfir for useful discussions. This research has been supported in part under Contract No. DE-AC02-76CH00016 with the U.S. Department of Energy and the BMFT.

[1] A. Bohr and B. R. Mottelson, *Nuclear Structure* (Benjamin, Reading, MA, 1975), Vol. I, p. 334.
[2] A. Wolf and R. F. Casten, Phys. Lett. B **280**, 1 (1992).
[3] A. Saha *et al.*, Phys. Lett. **132B**, 51 (1983).
[4] S. Raman *et al.*, At. Data Nucl. Data Tables **36**, 1 (1987).
[5] S. Raman *et al.*, Phys. Rev. C **37**, 805 (1988).
[6] J. N. Ginocchio and P. Van Isacker, Phys. Rev. C **33**, 365 (1986).
[7] R. F. Casten and D. D. Warner, Rev. Mod. Phys. **60**, 389 (1988).
[8] R. F. Casten and A. Wolf, Phys. Rev. C **35**, 1156 (1987).
[9] A. Wolf, O. Scholten, and R. F. Casten, Phys. Rev. C **43**, 2279 (1991).
[10] R. F. Casten, W. Frank, and P. von Brentano, Nucl. Phys. **A444**, 133 (1985).
[11] W. D. Hamilton, A. Irbäck, and J. P. Elliott, Phys. Rev. Lett. **53**, 2469 (1984).
[12] A. Wolf and R. F. Casten, Phys. Rev. C **36**, 851 (1987).
[13] P. Sala, A. Gelberg, and P. von Brentano, Z. Phys. A **323**, 281 (1986).
[14] I. Morrison and R. H. Spear, Phys. Rev. C **23**, 932 (1981).
[15] W. D. Hamilton, J. Phys. G **16**, 745 (1990).
[16] A. R. H. Subber *et al.*, J. Phys. G **13**, 807 (1987).
[17] A. F. Barfield and K. P. Lieb, Phys. Rev. C **41**, 1762

(1990).
[18] A. Giannatiempo *et al.*, Phys. Rev. C **44**, 1508 (1991).
[19] R. F. Casten *et al.*, Phys. Rev. Lett. **47**, 1433 (1981).
[20] K. Heyde *et al.*, Nucl. Phys. **A466**, 189 (1987).
[21] J. A. Cizewski and A. E. L. Dieperink, Phys. Lett. **164B**, 236 (1985).
[22] R. F. Casten, K. Heyde, and A. Wolf, Phys. Lett. B **208**, 33 (1988).
[23] A. Arima, T. Otsuka, F. Iachello, and I. Talmi, Phys. Lett. **66B**, 205 (1977).
[24] H. Harter, P. von Brentano, and A. Gelberg, Phys. Rev. C **34**, 1472 (1986); A. Leviatan, J. N. Ginocchio, and M. W. Kirson, Phys. Rev. Lett. **65**, 2853 (1990); J. N. Ginocchio, W. Frank, and P. von Brentano, Nucl. Phys. **A541**, 211 (1992).
[25] A. Novoselsky and I. Talmi, Phys. Lett. **160B**, 13 (1985).
[26] A. Richter, in *Proceedings of the International Nuclear Physics Conference,* edited by P. Blasi and R. A. Ricci (Tipografica Compositori, Bologna, 1983), Vol. 2, p. 189; D. Bohle, A. Richter, W. Steffen, A. E. L. Dieperink, N. Lo Iudice, F. Palumbo, and O. Scholten, Phys. Lett. **137B**, 27 (1984).
[27] J. N. Ginocchio, A. Leviatan, and M. W. Kirson, in *Capture Gamma-Ray Spectroscopy,* Proceedings of the Seventh International Symposium on Capture Gamma-Ray Spectroscopy and Related Topics, edited by R. W. Hoff, AIP Conf. Proc. No. 238 (AIP, New York, 1991), p. 82.